Cell Reports

Report

PD-1 Signaling Promotes Control of Chronic Viral Infection by Restricting Type-I-Interferon-Mediated Tissue Damage

Graphical Abstract

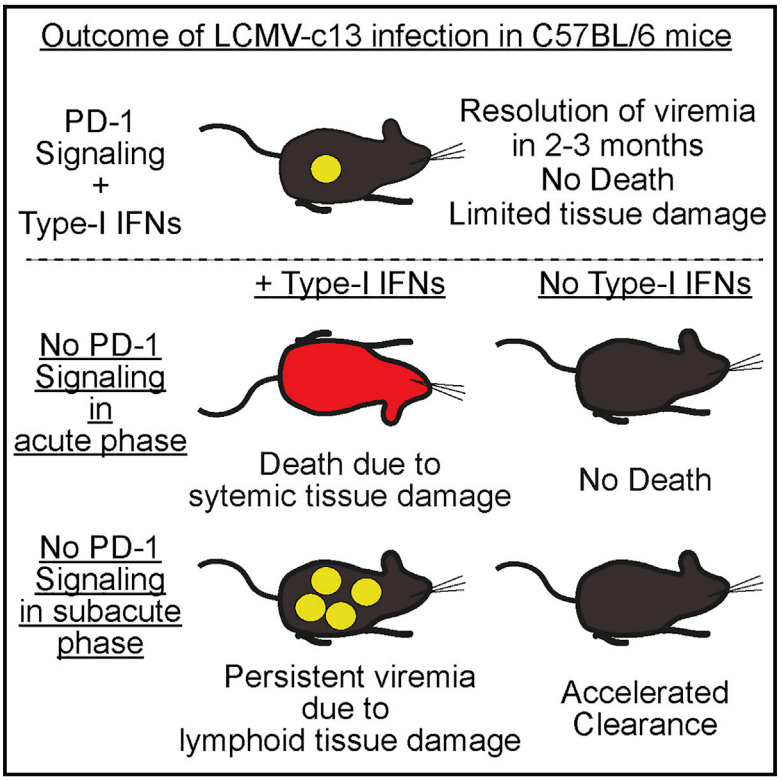

Highlights

- Host response to PD-1 blockade is timing dependent in LCMV-c13 infection
- PD-1 blockade in the subacute period leads to persistent viremia
- The impaired antiviral response results from lymphoid tissue damage by CD8 T cells
- Blocking IFNAR rescues LCMV-infected mice from immunopathology by PD-1 blockade

Authors

Saravanan Raju, Daniel J. Verbaro, Takeshi Egawa

Correspondence

egawat@wustl.edu

In Brief

Using stage-specific PD-1 blockade in LCMV-infected mice, Raju et al. uncover the requirement for PD-1-mediated suppression of CD8 T cells for durable immune response to chronic viral infection, as well as the requirement for IFNAR signaling in programming of CD8 T cells toward effectors that cause immunopathology.

Raju et al., 2019, Cell Reports *29*, 2556–2564
November 26, 2019
https://doi.org/10.1016/j.celrep.2019.10.092

CellPress

OPEN ACCESS
CellPress

Cell Reports
Report

PD-1 Signaling Promotes Control of Chronic Viral Infection by Restricting Type-I-Interferon-Mediated Tissue Damage

Saravanan Raju,[1] Daniel J. Verbaro,[1] and Takeshi Egawa[1,2,*]
[1]Department of Pathology and Immunology, Washington University School of Medicine, Saint Louis, MO 63110, USA
[2]Lead Contact
*Correspondence: egawat@wustl.edu
https://doi.org/10.1016/j.celrep.2019.10.092

SUMMARY

Immune responses are essential for pathogen elimination but also cause tissue damage, leading to disease or death. However, it is unclear how the host immune system balances control of infection and protection from the collateral tissue damage. Here, we show that PD-1-mediated restriction of immune responses is essential for durable control of chronic LCMV infection in mice. In contrast to responses in the chronic phase, PD-1 blockade in the subacute phase of infection paradoxically results in viral persistence. This effect is associated with damage to lymphoid architecture and subsequently decreases adaptive immune responses. Moreover, this tissue damage is type I interferon dependent, as sequential blockade of the interferon receptor and PD-1 pathways prevents immunopathology and enhances control of infection. We conclude that PD-1-mediated suppression is required as an immunoregulatory mechanism for sustained responses to chronic viral infection by antagonizing type-I interferon-dependent immunopathology.

INTRODUCTION

The host immune system responds to invading pathogens through a variety of effector mechanisms that not only control infection but also cause host damage (Rouse and Sehrawat, 2010). Reduction of pathogen burden occurs primarily through immune effector mechanisms, including expression of cytokines and cytotoxic molecules (Kägi et al., 1994; Samuel, 2001). However, elimination of pathogens often causes collateral tissue damage, referred to as immunopathology, leading to significant disease or death (Doherty and Zinkernagel, 1974; Graham et al., 2005; Zinkernagel, 2005). Several regulatory mechanisms prevent excessive immune activation and development of immunopathology, including expression of inhibitory receptors and cytokines, as well as the generation of regulatory immune cells (Chen and Flies, 2013; Josefowicz et al., 2012; Moore et al., 2001). Although immunoregulatory factors restrict effector responses, the long-term consequence of attenuated activity on pathogen control is unclear.

The inhibitory receptor PD-1 is rapidly upregulated following exposure of T cells to antigen (Ag) and remains high during experimental infection of mice with rapidly replicating *Lymphocytic choriomeningitis virus* (LCMV) strains, such as clone 13 (Ahn et al., 2018; Barber et al., 2006). High Ag load results in decreased CD8 T cell function, termed T cell "exhaustion," and a long-term viremia that is eventually resolved in a majority of immunocompetent mice (Matloubian et al., 1994; Moskophidis et al., 1993). A mechanistic link between PD-1-mediated inhibition of T cells and viral persistence is exemplified by the inhibition of the PD-1:PD-L1 interaction, which leads to "reinvigoration" of CD8 T cells and accelerates control of viremia (Barber et al., 2006; Lee et al., 2015). Thus, engagement of PD-1 signaling compromises viral control through attenuation of effector responses after CD8 T cells are exposed to high viral load. In contrast, infection of *Pdcd1*$^{-/-}$ or *Cd274*(encoding PD-L1)$^{-/-}$ mice with LCMV-c13 results in lethal immunopathology within several days after infection (Barber et al., 2006; Frebel et al., 2012), indicating that PD-1-dependent immune regulation is essential to restrict host damage. Thus, PD-1-mediated attenuation of antiviral responses by CD8 T cells is thought to be primarily an immunoregulatory mechanism by which the infected host minimizes tissue damage (Speiser et al., 2014), although the impact of the attenuated immunity on pathogen control remains unknown. These findings collectively imply that the consequence of PD-1-mediated regulation of immune responses depends on the context of host-microbe interactions, such as microenvironmental cues and inflammatory signals.

In this study, we sought to define the impact of PD-1 signaling on long-term viral control and the contexts that modulate its function in host-pathogen interactions. We found that loss of PD-1 signals during the early stages of chronic viral infection results in long-term viral persistence. Defective antiviral immunity resulted from atrophy of lymphoid tissues and global lymphopenia with marked loss of germinal center (GC) B cells due to excessive T cell responses. Intriguingly, a transient blockade of type I interferons (IFN-Is) not only reversed tissue damage caused by PD-1 blockade but also enhanced viral clearance in combination with a subsequent PD-1 blockade. Thus, functional outcomes of the engagement or blockade of the PD-1 pathway depend on inflammatory conditions established by IFN-Is, and thus, the PD-1 pathway must be engaged not only for host

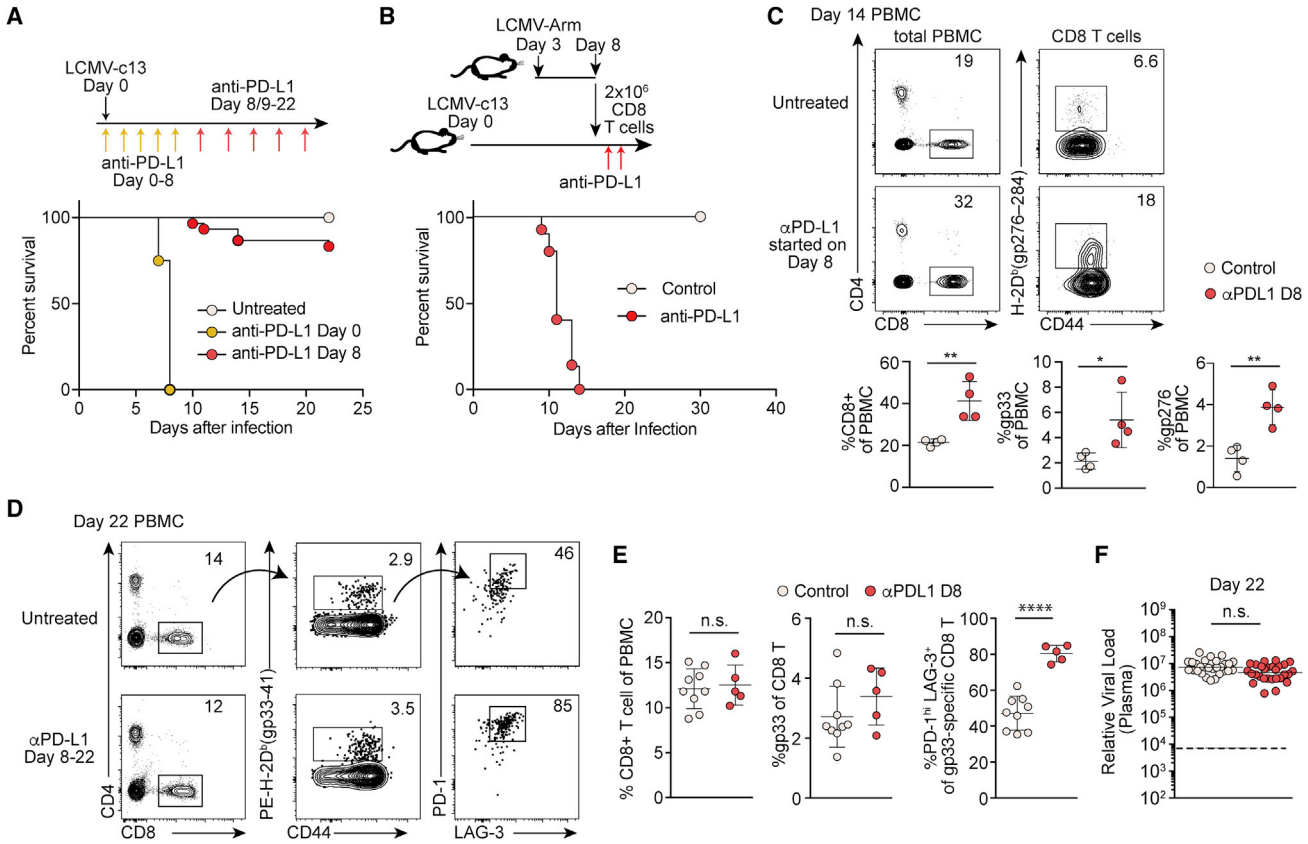

Figure 1. PD-1 Blockade at the Peak of Viremia Enhances CD8 T Cell Activation with No Immediate Impact on Viral Control

(A) Survival LCMV-c13-infected B6 mice following anti-PD-L1 treatment. n = 25 (control), n = 6 (days 0–8), and n = 30 (days 8–22) pooled from 3 experiments.

(B) Survival of LCMV-c13-infected B6 mice after adoptive transfer of unexhausted LCMV-specific CD8 T cells and treatment with anti-PD-L1 or isotype control. Data are from 3 experiments.

(C) Expression of CD4, CD8, CD44, and LCMV-gp276-specific T cell receptor (TCR) in peripheral blood mononuclear cells (PBMCs) from control and anti-PD-L1-treated mice on 14 dpi with LCMV-c13 infection. Representative plots are shown with mean ± SD from 3 experiments.

(D and E) Expression of CD4, CD8, CD44, PD-1, LAG-3, and LCMV-gp33-specific TCR in PBMCs on 22 dpi. Representative plots (D) and mean ± SD from 2 experiments (E) are shown.

(F) Plasma viral RNA load in LCMV-c13-infected mice on 22 dpi. Data pooled from 5 experiments are shown with median. The statistical difference was tested by the Mann-Whitney U test.

See also Figure S1.

protection against immunopathology but also for durable antiviral immunity.

RESULTS

PD-1 Blockade at the Peak of Viremia Enhances CD8 T Cell Activation with No Immediate Impact on Viral Control

Cd274$^{-/-}$ mice die from immunopathology by infection with the chronic LCMV-c13, but not the acute LCMV-Armstrong (LCMV-Arm) strain (Barber et al., 2006). To determine whether high viral load is sufficient to induce the lethal immunopathology in the absence of PD-1 signaling, we infected C57BL/6 (B6) mice with LCMV-c13 and blocked PD-1 by injecting anti-PD-L1 monoclonal antibody (mAb) on day 8 post-infection (dpi), corresponding to the peak of viremia (Wherry et al., 2003). As a control, we infected B6 mice with LCMV-c13 and treated with anti-PD-L1 at the time of infection, recapitulating lethal immunopathology as shown using *Cd274*$^{-/-}$ mice (Figure 1A; Barber et al., 2006; Frebel et al., 2012). Depletion of CD8 T cells prior to infection completely rescued the mice from death, although depletion of CD4 T cells had little impact on their survival, confirming CD8 T-cell-dependent immunopathology (Figure S1A; Frebel et al., 2012). Although overriding PD-1-mediated suppression during the initial stages after infection achieved expansion of Ag-specific CD8 T cells on 5 dpi, it had little impact on the establishment of high viremia (Figures S1B–S1D), suggesting a minimal role of PD-1 in controlling virus in this context.

In marked contrast, the majority of mice survived when anti-PD-L1 treatment started on 8 dpi (Figure 1A), indicating that high viral load is insufficient to cause death of the infected mice. To rule out the possibility that the lack of death resulted from resistance of target tissues or reduced Ag presentation, we transferred unexhausted CD8 T cells harvested from

LCMV-Arm-infected mice into LCMV-c13-infected mice and subsequently treated the recipient mice with anti-PD-L1. All LCMV-c13-infected recipient mice died quickly after anti-PD-L1 treatment (Figure 1B), indicating that the resistance to lethal pathology of mice treated with anti-PD-L1 on 8–22 dpi is independent of T-cell-extrinsic resistance of the infected animals.

The increased frequency of total and LCMV-specific CD8 T cells in the peripheral blood on 14 dpi in mice with anti-PD-L1 treatment started on 8 dpi indicated that virus-specific CD8 T cells are suppressed by PD-1 signaling during this period (Figure 1C). However, the increase in CD8 T cells was no longer observed on 22 dpi with expression of PD-1 and LAG-3 by LCMV-specific CD8 T cells being elevated in anti-PD-L1-treated compared with control antibody-treated or untreated mice (Figures 1D and 1E). PD-1 blockade has been shown to promote pathogen clearance in certain infection models, including LCMV-c13 infection (Barber et al., 2006; Bhadra et al., 2011; Fuller et al., 2013). However, plasma viral titers were unchanged on day 22 dpi (Figure 1F). These results indicate that engagement of the PD-1 pathway during the acute and subacute phases has little immediate impact on control of viral infection.

PD-1 Signaling Protects Host from Sustained Immunopathology in Lymphoid Organs

Although the majority of LCMV-infected mice treated with anti-PD-L1 initiated on 8 dpi survived, we found a significant delay in recovery of body weight, suggesting that PD-1 blockade during this period causes non-lethal immunopathology (Figure S2A). Lymphoid organs are transiently disrupted following LCMV-c13 infection due predominantly to T-cell-mediated tissue damage (Müller et al., 2002; Teijaro et al., 2013; Wilson et al., 2013; Zinkernagel et al., 1999). We thus determined whether excessive loss of the integrity of lymphoid organs, presumably impacting subsequent durable immunity, is a direct consequence of PD-1 blockade. Indeed, spleen sizes and splenocyte numbers in anti-PD-L1-treated mice were significantly reduced compared to controls (Figures 2A and 2B). Histological analyses of spleens on 14 and 22 dpi revealed smaller B cell follicles and disrupted red and white pulp boundaries in anti-PD-L1-treated animals (Figures 2C and S2B). This tissue damage in the spleen was CD8 T cell dependent because it was prevented by depletion of CD8 T cells prior to infection (Figure S2C). Frequencies of LCMV-specific CD8 T cells, including "terminally exhausted" PD-1^+ TIM-3^+ cells and stem-cell-like PD-1^+ TCF-1^+ cells (Im et al., 2016; Utzschneider et al., 2016; Wu et al., 2016), were similar in control and treated mice (Figures 2D and 2E). However, absolute numbers of these populations were diminished in proportion to reductions in spleen size and cellularity (Figure 2E).

It has now become clear that the consequences of loss of PD-1 signaling differ depending on contexts in which the signal is blocked. Although the blockade at later time points in LCMV infection or in the tumor microenvironment enhances CD8 T cell responses, its constitutive loss paradoxically leads to more pronounced cell-intrinsic dysfunction of CD8 T cells (Barber et al., 2006; Odorizzi et al., 2015). To determine whether intrinsic CD8 T cell function is altered by PD-1 blockade during the subacute period, we analyzed cytokine production *ex vivo* and proliferative capacity of CD8 T cells *in vivo* by adoptive transfer to congenic mice followed by LCMV-c13 infection. Immediately following blockade of PD-L1, we detected increased frequencies of tumor necrosis factor alpha (TNF-α)$^+$ interferon (IFN)-γ^+ co-producing CD8 T cells *ex vivo* as well as an increased frequency of Ki-67^+ LCMV-specific CD8 T cells (Figures 2F and 2G), suggesting PD-1 blockade started on 8 dpi resulted in enhanced activity of Ag-specific CD8 T cells. Additionally, adoptively transferred PD-1^+ CD8 T cells from control or anti-PD-L1-treated mice were capable of comparable secondary expansion in the recipient mice (Figure 2H), indicating that Ag-specific CD8 T cells preserved polyfunctionality and proliferative capacity, regardless of PD-1 blockade during this period. These results suggest that the decreased overall CD8 T cell response in the treated mice is secondary to tissue damage in lymphoid organs caused by CD8 T cells.

CD8 T cells also directly target Ag-specific B cells in LCMV infection and thus impair antibody responses (Moseman et al., 2016). We hypothesized PD-1 blockade exacerbates CD8 T-cell-dependent cytotoxicity to B cells. Consistently, despite comparable frequencies of CD8 T cells and total B220^+ B cells, we observed a significant reduction in the frequencies and numbers of GL7^+ Fas$^+$ GC B cells known to be directly infected by LCMV (Moseman et al., 2016) as well as in anti-LCMV IgG2c titers (Figures 2I and 2J). Although PD-1 blockade could also act directly on B cells and cause their death by hyperactivation, we did not detect PD-1 expression on B cells at this stage of infection, making this explanation unlikely (Figure S2D). Moreover, depletion of CD8 T cells prior to infection restored GC B cell numbers and anti-LCMV IgG2c titers (Figures S2E and S2F), indicating that the GC B cell reduction was mediated by Ag-specific killing by uninhibited CD8 T cells. These data collectively indicate that PD-1 signaling during the subacute stage of LCMV infection protects hosts from excess tissue damage, particularly in the lymphoid organs that provide a microenvironment for proper adaptive immune responses. Thus, engagement of the PD-1 pathway may be an essential component of protective immunity to control persistent viral infection targeting lymphoid organs.

Engagement of PD-1/PD-L1 Is Essential for Control of Chronic LCMV Infection

We have shown that PD-1 is necessary to prevent tissue damage with no immediate impact on viral control. We thus hypothesized that insufficient adaptive immunity resulting from the defective lymphoid tissue integrity impairs long-term control of virus. Accordingly, we conducted a longitudinal analysis of viremia using different regimens of PD-1 blockade. As demonstrated previously (Barber et al., 2006), PD-1 blockade late in the infection, initiated on 23 dpi, accelerated resolution of viremia, with viral RNA undetectable by 50 dpi (Figure 3A, blue dots). In sharp contrast, PD-1 blockade initiated on 8 dpi impaired viral control with a majority of infected mice exhibiting viral persistence (Figure 3A, red dots). Thus, PD-1 engagement in the subacute phase of infection, after T cell priming and initial clonal expansion, is required to preserve durable antiviral responses.

To further delineate the effects of a temporary PD-1 blockade on 8–22 dpi, we first examined how function of Ag-specific CD8 T cells was impacted. It has been shown that loss of PD-1

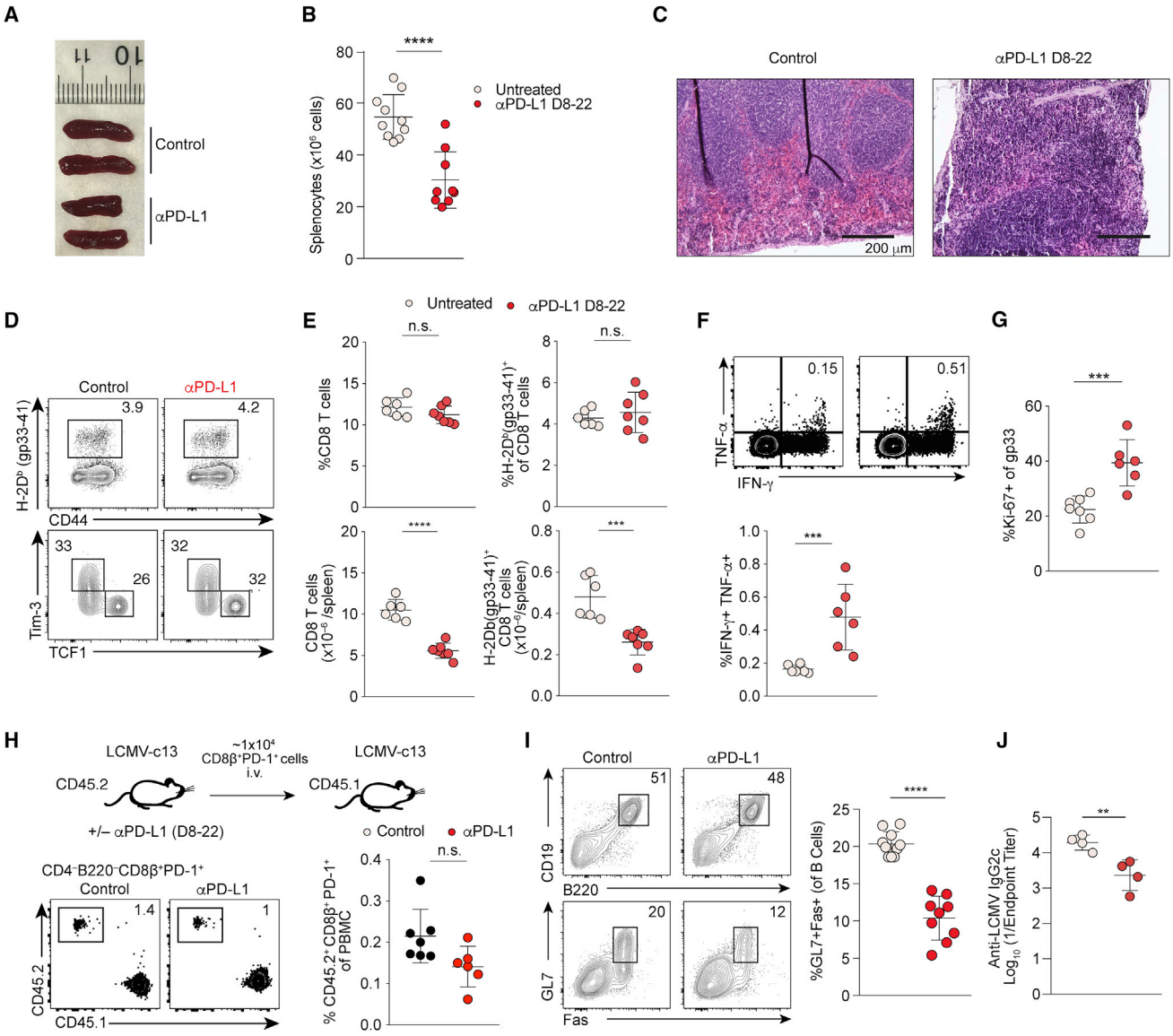

Figure 2. PD-1 Blockade at the Peak of Viral Load Results in Reduced Spleen Sizes and Pan-lymphopenia

(A) Gross images of spleens from control and anti-PD-L1-treated mice on 22 dpi.

(B) Splenocyte counts of control and anti-PD-L1-treated mice on 22 dpi. n > 8 mice per group, shown by mean and SD.

(C) H&E staining of spleen sections from control and day 8–22 anti-PD-L1-treated mice on 22 dpi. Scale bars, 200 μm. Representative images of 6 mice per group are shown.

(D) Expression of CD44 and LCMV-gp33-specific TCR of total splenocytes and expression of TCF-1 and TIM-3 by LCMV-gp33-specific CD8 T cells in control and anti-PD-L1-treated mice on 22 dpi.

(E) Statistical analysis of frequencies and absolute numbers of the indicated cell populations pooled from 2 experiments. n = 4–6 mice per group.

(F) Expression of IFN-γ and TNF-α by splenocytes from LCMV-c13-infected control and anti-PD-L1-treated B6 mice following stimulation with the gp276-284 peptide. Representative data from 2 experiments are shown with mean ± SD; n = 4.

(G) Expression of Ki-67 by gp33-specific CD8 T cells.

(H) Frequencies of CD45.2 PD-1$^+$ donor CD8 T cells in PBMCs of CD45.1-recipient mice that received PD-1$^+$ CD8 T cells from LCMV-c13-infected anti-PD-L1-treated B6 mice and subsequently challenged with LCMV-c13. Data are pooled from two experiments.

(I) Expression of Fas and GL7 expression in B220$^+$ splenocytes from control and anti-PD-L1-treated mice. Data from 2 experiments are shown with mean and SD.

(J) Anti-LCMV IgG2c antibody titers on 22 dpi.

See also Figure S2.

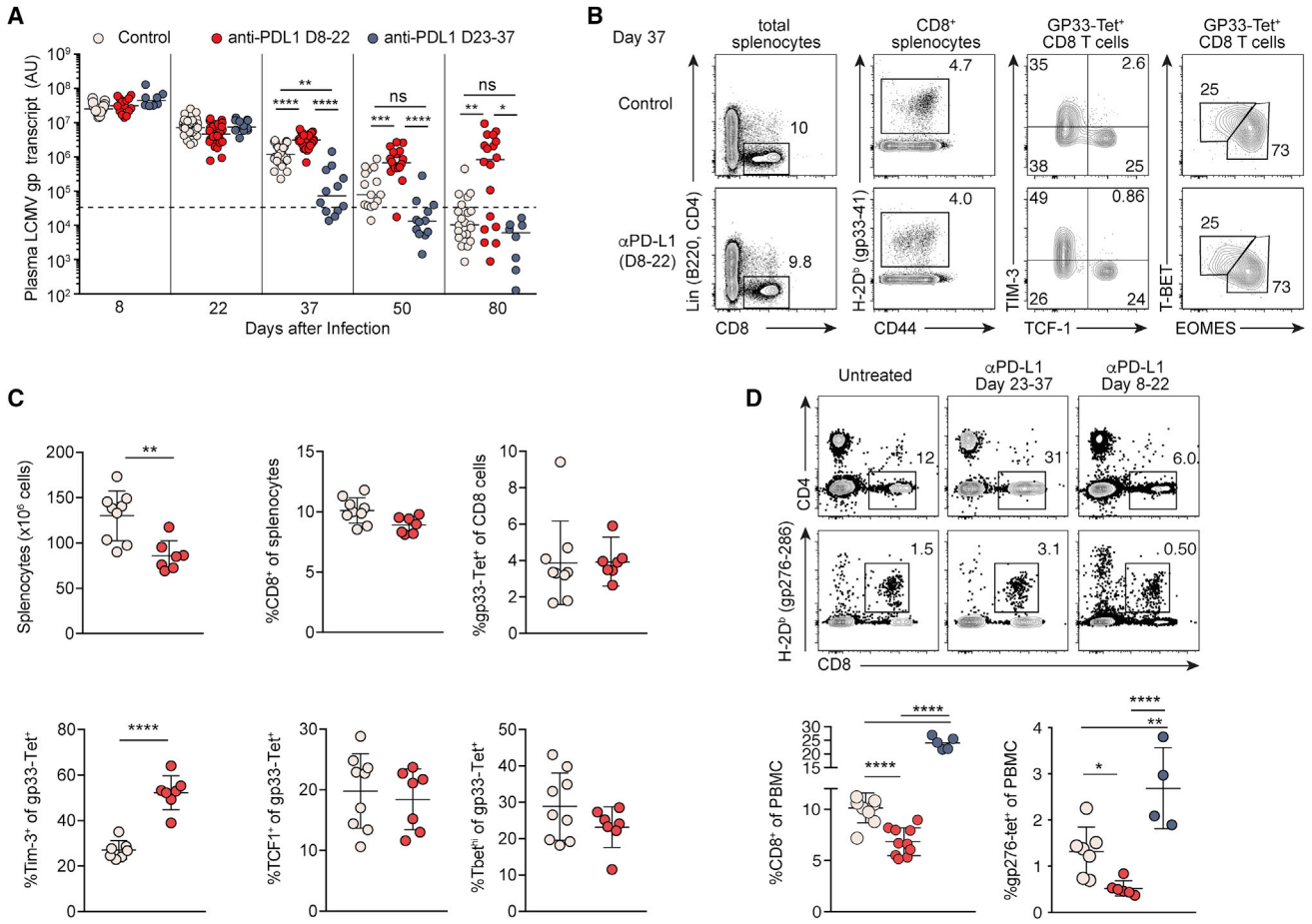

Figure 3. Engagement of PD-1 in the Subacute Phase Is Required for Durable Control of LCMV Infection

(A) Plasma viral RNA load in LCMV-c13-infected B6 mice treated with anti-PD-L1 on 8–22 dpi (red dots, same as Figure 1) or 23–37 dpi (blue dots). Data are pooled from 5 experiments shown with median.

(B–D) Expression of CD4, CD8, CD44, PD-1, LAG3, and LCMV-gp33-specific TCR by splenocytes (B and C) and peripheral blood mononuclear cells (D) on day 37 of LCMV-c13 infection. Representative plots are shown with median ± SD from at least 2 experiments.

signaling depletes T-bet$^+$ CD8 T cells, resulting in defective antiviral responses (Odorizzi et al., 2015). To this end, similar to analysis on 22 dpi, frequencies of LCMV-specific CD8 T cells, including those of PD-1$^+$ TCF-1$^+$ and T-bet$^+$ CD8 T cells, were comparable between 8–22 dpi treated and control groups in the spleen on 37 dpi (Figures 3B and 3C). However, expression of TIM-3 by Ag-specific CD8 T cells in the spleen was increased in the treated mice (Figures 3B and 3C), suggesting an accumulation of severely exhausted cells due to the changes in the microenvironment. This change of CD8 T cells in the spleen was reflected by more pronounced reduction of both total and LCMV-specific CD8 T cells in the peripheral blood (Figure 3D). Thus, it is likely that the decline in CD8 T cells and diminished anti-LCMV antibody responses led to defective viral control in mice treated with anti-PD-L1 between 8–22 dpi. Together, our results indicate that engagement of the PD-1 pathway in the face of persistent Ag is essential for durable antiviral responses by generating requisite numbers of adaptive immune cells through the maintenance of lymphoid tissue integrity.

IFN-Is Are Required for Anti-PD-L1-Mediated Immunopathology

Our results demonstrate the requirement of PD-1 signaling for protecting the host from tissue damage that compromises antiviral responses. However, immunopathology preferentially occurred during early time points in the infection, potentially due to elevated inflammatory cytokines. Among the cytokines induced upon viral infection, IFN-Is are transiently produced through by plasmacytoid dendritic cells (pDCs) and other myeloid cells upon infection by LCMV-c13 (Macal et al., 2012; Teijaro et al., 2013; Wang et al., 2012; Wilson et al., 2013; Ng et al., 2015). The expression of IFN-Is peaks in the acute stage and would thus be consistent with their roles in enhancing immunopathology following anti-PD-L1 treatment in the acute phase (Baccala et al., 2014; Oldstone et al., 2018). To first test whether IFN-Is were required for lethal immunopathology in LCMV-c13-infected mice resulting from PD-1 blockade, we combined administration of blocking mAbs against interferon alpha/beta receptor 1 (IFNAR) immediately before infection

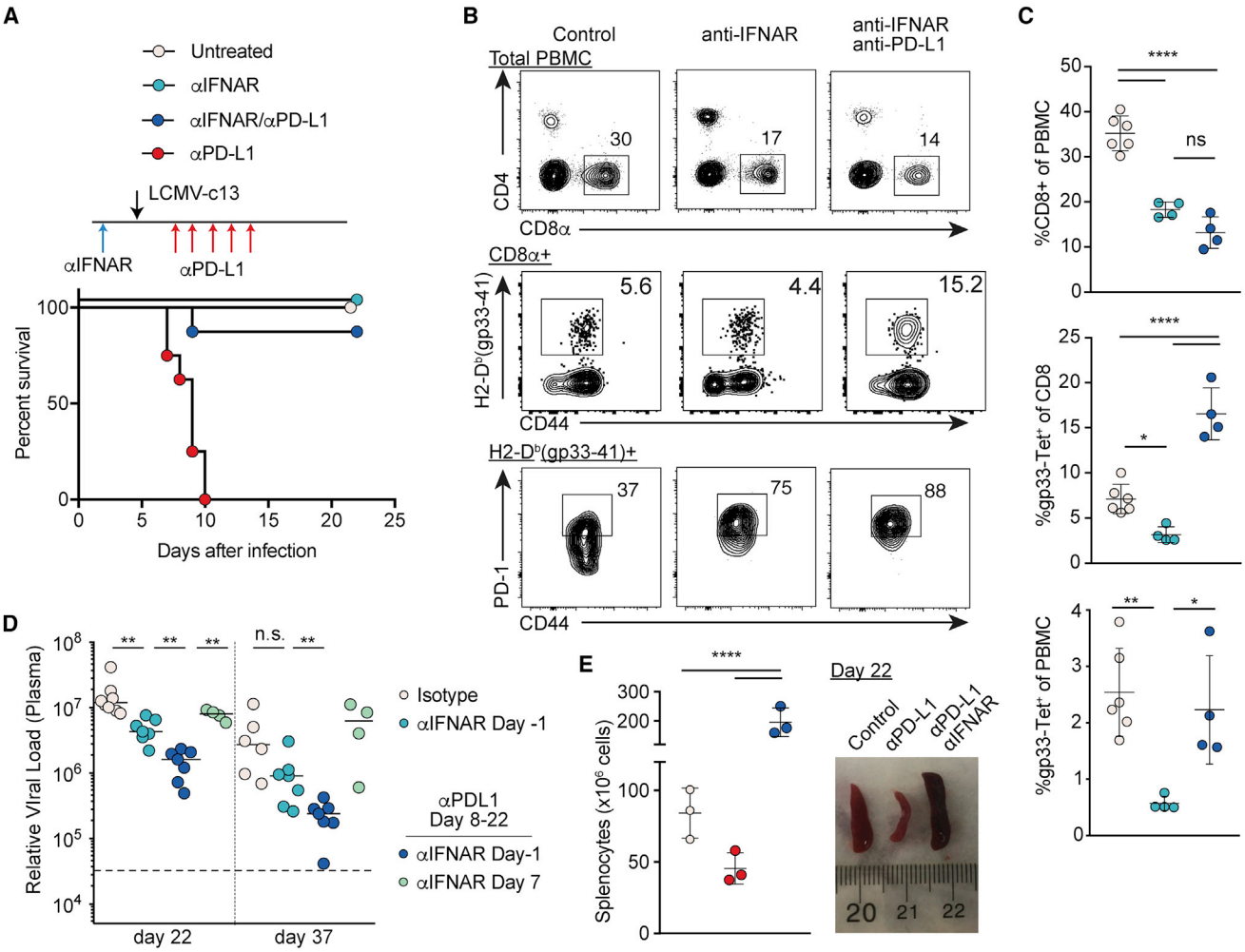

Figure 4. Type I Interferon Receptor Blockade Rescues Immunopathology Caused by Loss of PD-1 Signaling in LCMV-Infected Mice

(A) Survival of LCMV-c13-infected B6 mice treated with anti-IFNAR 1 day prior to infection, anti-PD-L1 (days 0, 2, 4, 6, and 8), or both. Data pooled from 3 experiments with n > 6 mice per group are shown.

(B and C) Frequencies of total CD8 T cells, LCMV-gp33-specific CD8 T cells, and PD-1$^+$ cells in indicated PBMC populations on 8 dpi in LCMV-c13-infected B6 mice with indicated treatment. Representative plots (B) with mean ± SD from 2 experiments (C) are shown.

(D) Plasma LCMV viral RNA load in LCMV-c13-infected B6 mice with indicated treatment from 2 experiments shown with median.

(E) Macroscopic images of spleen and splenocyte counts of LCMV-c-13-infected B6 mice with indicated treatment as in (A) on 22 dpi. Data from two experiments are shown.

See also Figures S3 and S4.

(day −1) and PD-L1 on 0–8 dpi. In striking contrast to mice treated with anti-PD-L1 alone, almost all infected mice were rescued from death by the co-treatment (Figure 4A), indicating that IFN-Is enhance effector function of Ag-specific CD8 T cells.

We next examined how loss of IFNAR signaling impacted the CD8 T cell response to LCMV-c13 infection. We found reduced frequencies of total and LCMV-specific CD8 T cells in peripheral blood on 8 dpi in anti-IFNAR-treated mice (Figure 4B). This diminished CD8 T cell expansion was independent of natural killer (NK)-cell-dependent cytotoxicity, as CD8 T cell frequencies remained unchanged with depletion of NK cells (Crouse et al., 2014; Madera et al., 2016; Xu et al., 2014; Figure S3A). In *Ifnar1*$^{-/-}$ mice, splenocyte counts were increased by two-fold, consistent with diminished CD8 T-cell-mediated tissue damage, although total and LCMV-specific CD8 T cell numbers were reduced (Figures S3B–S3E). Among LCMV-specific CD8 T cells, we observed skewed differentiation into TCF-1$^+$ memory-like CD8 T cells over TIM-3$^+$ effector/exhausted cells (Figures S3B–S3E), consistent with a previous study (Wu et al., 2016). These results suggest that differentiation of activated CD8 T cells into effectors is suppressed in the absence of IFNAR signaling. In addition, LCMV-specific CD8 T cells deprived of IFNAR signaling expressed substantially higher PD-1 compared to control CD8 T cells (Figure 4B) and therefore may be more sensitive to PD-L1-mediated suppression.

Consistently, additional blockade of PD-1 signaling rescued the reduction in LCMV-specific CD8 T cells without impacting total CD8 T cell frequencies (Figures 4B and 4C).

We next sought to establish which cellular compartments IFN-Is target to cause immunopathology. Bone marrow (BM) chimeras reconstituted with *Ifnar1*$^{-/-}$ hematopoietic cells died following LCMV-c13 infection and anti-PD-L1 treatment with similar kinetics to control chimeric mice reconstituted with wild-type (WT) BM cells (Figure S4A). Although *Ifnar1*$^{-/-}$ host mice reconstituted with *Ifnar1*$^{-/-}$ hematopoietic cells were resistant to PD-1-blockade-mediated death as expected, *Ifnar1*$^{-/-}$ hosts reconstituted with WT BM cells also succumbed to PD-1 blockade following LCMV-c13 infection (Figure S4B). These results collectively indicate that IFN-Is program enhanced CD8 T cell effector responses by acting on both non-hematopoietic and hematopoietic cells and in part by restricting induction of PD-1 in activated CD8 T cells to desensitize them to PD-L1-mediated suppression.

To determine whether early PD-1 blockade can promote control of infection in the absence of excess tissue damage, we tracked antiviral responses following anti-IFNAR and anti-PD-L1 treatment. As shown previously (Teijaro et al., 2013; Wilson et al., 2013), anti-IFNAR alone on day −1 prior to infection accelerated resolution of viremia compared to control (Figure 4D). The viral control was further enhanced by combination of anti-IFNAR on day −1 with anti-PD-L1 on 8 dpi. In contrast, anti-IFNAR administration on 7 dpi, at which time IFN-Is are already undetectable in serum (Macal et al., 2012; Teijaro et al., 2013; Wang et al., 2012; Wilson et al., 2013), had no effect (Figure 4D). Consistently, atrophy of the spleen caused by anti-PD-L1 was completely rescued in mice co-treated with anti-IFNAR and anti-PD-L1 (Figure 4E). These results suggest IFN-Is as a target to tune the outcomes of immune checkpoint blockade.

DISCUSSION

Our data demonstrate a critical, temporal function of PD-1 in the regulation of host immunity against persistent infections. PD-1 is a major inhibitory receptor that causes attenuated CD8 T cell responses to some infections and tumors. Blockade of the PD-1/PD-L1 interaction to restore function of exhausted CD8 T cells was originally demonstrated using a mouse chronic LCMV infection model and has now been applied broadly as a cancer immunotherapy in humans. However, the biological significance of PD-1-mediated suppression on long-term control of persistent viral infection is understudied. We now demonstrate that PD-1-mediated restriction of T cell responses is beneficial for control of chronic infection.

Immunopathology in the LCMV-c13 infection model is a consequence of abundant and broad expression of viral Ag across different cell types. LCMV is a non-cytopathic virus, and the pathogenesis of LCMV infection is predominantly host T cell response dependent, as is the case with some viral infections in humans, such as hepatitis B virus (HBV), HCV, and HIV infections. Context-dependent PD-1-mediated protection through restriction of immunopathology may be beneficial to establish durable immunity against those infections, although the benefit of restraining host T cell responses may not be applicable to all viral infections. Constitutive absence of PD-1 signal causes severe exhaustion of CD8 T cells in a cell-intrinsic manner (Odorizzi et al., 2015). In contrast, our results show the requirement for PD-1 to preserve CD8 T cell responses in a T-cell-extrinsic manner and thus reveal the additional role of immune regulation in durable antiviral immunity. Collectively, restriction of CD8 T cell function by PD-1 or acquisition of the exhausted state is a host protective mechanism in response to persistent Ag, for which long-term durable immunity is prioritized at the expense of immediate immune responses.

Our results also show that IFN-Is enhance immunopathology in the setting of PD-1/PD-L1 deficiency. Sequential blockade of IFNAR and PD-1 signaling synergistically improved control of LCMV infection, further supporting our conclusion that preventing initial immunopathology is critical for overall antiviral responses, even if it temporarily compromises viral control. Although IFNAR is broadly expressed in both hematopoietic and non-hematopoietic compartments, its expression in either compartment was sufficient to cause lethal immunopathology in LCMV-c13-infected mice depleted of PD-1 signaling. IFNAR signaling thus likely contributes to maximizing CD8 T cell responses through multiple mechanisms, including effector differentiation and modulation of PD-1 expression by CD8 T cells. Although blockade of IFNAR signaling enhances control of persistent LCMV infection (Teijaro et al., 2013; Wilson et al., 2013), the therapeutic effects appear to be mediated by regulation of CD8 T cells and preservation of host immune functions, similar to PD-1-mediated suppression, rather than direct enhancement of T cell function. This conclusion is supported by protection of LCMV-specific B cells by IFNAR blockade (Fallet et al., 2016; Moseman et al., 2016). The IFN-I pathway could be a potential target for modulation of immunotherapies against infections and cancer beyond its direct effect on the virus or transformed cells.

STAR★METHODS

Detailed methods are provided in the online version of this paper and include the following:

- KEY RESOURCES TABLE
- LEAD CONTACT AND MATERIALS AVAILABILITY
- EXPERIMENTAL MODEL AND SUBJECT DETAILS
  - Mice
- METHOD DETAILS
  - Mouse Infection and Viral Load Quantification
  - Antibody treatments
  - Histology
  - Cell Preparation, Staining, and Flow Cytometry
  - Anti-LCMV antibody ELISA
- QUANTIFICATION AND STATISTICAL ANALYSIS
- DATA AND CODE AVAILABILITY

SUPPLEMENTAL INFORMATION

Supplemental Information can be found online at https://doi.org/10.1016/j.celrep.2019.10.092.

ACKNOWLEDGMENTS

We thank M. Colonna and M. Cella for LCMV stocks; M.S. Diamond for *Ifnar1*$^{-/-}$ mice; J. Boon, C. Fujii, and M. Holmgren for technical support; and C.-S. Hsieh, E.M. Oltz, and E. Tonc for discussion and critical reading of the manuscript. This study was supported by United States National Institutes of Health (NIH) grants R01AI130152-01A1 and R03AI139875-01 (to T.E.), T32HL007317 (to S.R.), and T32GM007200 (to S.R. and D.J.V.). T.E. is a Scholar of the Leukemia and Lymphoma Society (https://www.lls.org, United States). The ORCID for T.E. is 0000-0001-7489-1051.

AUTHOR CONTRIBUTIONS

S.R. and T.E. designed the study. S.R. and D.J.V. conducted experiments. S.R. and T.E. interpreted results and wrote the manuscript.

DECLARATION OF INTERESTS

The authors declare no competing interests.

Received: February 25, 2019
Revised: October 3, 2019
Accepted: October 22, 2019
Published: November 26, 2019

REFERENCES

Ahn, E., Araki, K., Hashimoto, M., Li, W., Riley, J.L., Cheung, J., Sharpe, A.H., Freeman, G.J., Irving, B.A., and Ahmed, R. (2018). Role of PD-1 during effector CD8 T cell differentiation. Proc. Natl. Acad. Sci. USA *115*, 4749–4754.

Baccala, R., Welch, M.J., Gonzalez-Quintial, R., Walsh, K.B., Teijaro, J.R., Nguyen, A., Ng, C.T., Sullivan, B.M., Zarpellon, A., Ruggeri, Z.M., et al. (2014). Type I interferon is a therapeutic target for virus-induced lethal vascular damage. Proc. Natl. Acad. Sci. USA *111*, 8925–8930.

Barber, D.L., Wherry, E.J., Masopust, D., Zhu, B., Allison, J.P., Sharpe, A.H., Freeman, G.J., and Ahmed, R. (2006). Restoring function in exhausted CD8 T cells during chronic viral infection. Nature *439*, 682–687.

Bhadra, R., Gigley, J.P., Weiss, L.M., and Khan, I.A. (2011). Control of Toxoplasma reactivation by rescue of dysfunctional CD8+ T-cell response via PD-1-PDL-1 blockade. Proc. Natl. Acad. Sci. USA *108*, 9196–9201.

Chen, L., and Flies, D.B. (2013). Molecular mechanisms of T cell co-stimulation and co-inhibition. Nat. Rev. Immunol. *13*, 227–242.

Chou, C., Verbaro, D.J., Tonc, E., Holmgren, M., Cella, M., Colonna, M., Bhattacharya, D., and Egawa, T. (2016). The transcription factor AP4 mediates resolution of chronic viral infection through amplification of germinal center B cell responses. Immunity *45*, 570–582.

Crouse, J., Bedenikovic, G., Wiesel, M., Ibberson, M., Xenarios, I., Von Laer, D., Kalinke, U., Vivier, E., Jonjic, S., and Oxenius, A. (2014). Type I interferons protect T cells against NK cell attack mediated by the activating receptor NCR1. Immunity *40*, 961–973.

Doherty, P.C., and Zinkernagel, R.M. (1974). T-cell-mediated immunopathology in viral infections. Transplant. Rev. *19*, 89–120.

Fallet, B., Narr, K., Ertuna, Y.I., Remy, M., Sommerstein, R., Cornille, K., Kreutzfeldt, M., Page, N., Zimmer, G., Geier, F., et al. (2016). Interferon-driven deletion of antiviral B cells at the onset of chronic infection. Sci. Immunol. *1*, eaah6817.

Frebel, H., Nindl, V., Schuepbach, R.A., Braunschweiler, T., Richter, K., Vogel, J., Wagner, C.A., Loffing-Cueni, D., Kurrer, M., Ludewig, B., and Oxenius, A. (2012). Programmed death 1 protects from fatal circulatory failure during systemic virus infection of mice. J. Exp. Med. *209*, 2485–2499.

Fuller, M.J., Callendret, B., Zhu, B., Freeman, G.J., Hasselschwert, D.L., Satterfield, W., Sharpe, A.H., Dustin, L.B., Rice, C.M., Grakoui, A., et al. (2013). Immunotherapy of chronic hepatitis C virus infection with antibodies against programmed cell death-1 (PD-1). Proc. Natl. Acad. Sci. USA *110*, 15001–15006.

Graham, A.L., Allen, J.E., and Read, A.F. (2005). Evolutionary causes and consequences of immunopathology. Ann. Rev. Ecol. Evol. Syst. *36*, 373–397.

Im, S.J., Hashimoto, M., Gerner, M.Y., Lee, J., Kissick, H.T., Burger, M.C., Shan, Q., Hale, J.S., Lee, J., Nasti, T.H., et al. (2016). Defining CD8+ T cells that provide the proliferative burst after PD-1 therapy. Nature *537*, 417–421.

Josefowicz, S.Z., Lu, L.-F., and Rudensky, A.Y. (2012). Regulatory T cells: mechanisms of differentiation and function. Annu. Rev. Immunol. *30*, 531–564.

Kägi, D., Ledermann, B., Bürki, K., Seiler, P., Odermatt, B., Olsen, K.J., Podack, E.R., Zinkernagel, R.M., and Hengartner, H. (1994). Cytotoxicity mediated by T cells and natural killer cells is greatly impaired in perforin-deficient mice. Nature *369*, 31–37.

Lee, J., Ahn, E., Kissick, H.T., and Ahmed, R. (2015). Reinvigorating exhausted T cells by blockade of the PD-1 pathway. For. Immunopathol. Dis. Therap. *6*, 7–17.

Macal, M., Lewis, G.M., Kunz, S., Flavell, R., Harker, J.A., and Zúñiga, E.I. (2012). Plasmacytoid dendritic cells are productively infected and activated through TLR-7 early after arenavirus infection. Cell Host Microbe *11*, 617–630.

Madera, S., Rapp, M., Firth, M.A., Beilke, J.N., Lanier, L.L., and Sun, J.C. (2016). Type I IFN promotes NK cell expansion during viral infection by protecting NK cells against fratricide. J. Exp. Med. *213*, 225–233.

Matloubian, M., Concepcion, R.J., and Ahmed, R. (1994). CD4+ T cells are required to sustain CD8+ cytotoxic T-cell responses during chronic viral infection. J. Virol. *68*, 8056–8063.

McCausland, M.M., and Crotty, S. (2008). Quantitative PCR technique for detecting lymphocytic choriomeningitis virus in vivo. J. Virol. Methods *147*, 167–176.

Moore, K.W., de Waal Malefyt, R., Coffman, R.L., and O'Garra, A. (2001). Interleukin-10 and the interleukin-10 receptor. Annu. Rev. Immunol. *19*, 683–765.

Moseman, E.A., Wu, T., de la Torre, J.C., Schwartzberg, P.L., and McGavern, D.B. (2016). Type I interferon suppresses virus-specific B cell responses by modulating CD8^{+} T cell differentiation. Sci. Immunol. *1*, eaah3565.

Moskophidis, D., Lechner, F., Pircher, H., and Zinkernagel, R.M. (1993). Virus persistence in acutely infected immunocompetent mice by exhaustion of antiviral cytotoxic effector T cells. Nature *362*, 758–761.

Müller, S., Hunziker, L., Enzler, S., Bühler-Jungo, M., Di Santo, J.P., Zinkernagel, R.M., and Mueller, C. (2002). Role of an intact splenic microarchitecture in early lymphocytic choriomeningitis virus production. J. Virol. *76*, 2375–2383.

Ng, C.T., Sullivan, B.M., Teijaro, J.R., Lee, A.M., Welch, M., Rice, S., Sheehan, K.C.F., Schreiber, R.D., and Oldstone, M.B.A. (2015). Blockade of interferon beta, but not interferon alpha, signaling controls persistent viral infection. Cell Host Microbe *17*, 653–661.

Odorizzi, P.M., Pauken, K.E., Paley, M.A., Sharpe, A., and Wherry, E.J. (2015). Genetic absence of PD-1 promotes accumulation of terminally differentiated exhausted CD8+ T cells. J. Exp. Med. *212*, 1125–1137.

Oldstone, M.B.A., Ware, B.C., Horton, L.E., Welch, M.J., Aiolfi, R., Zarpellon, A., Ruggeri, Z.M., and Sullivan, B.M. (2018). Lymphocytic choriomeningitis virus clone 13 infection causes either persistence or acute death dependent on IFN-1, cytotoxic T lymphocytes (CTLs), and host genetics. Proc. Natl. Acad. Sci. USA *115*, E7814–E7823.

Raju, S., Kometani, K., Kurosaki, T., Shaw, A.S., and Egawa, T. (2018). The adaptor molecule CD2AP in CD4 T cells modulates differentiation of follicular helper T cells during chronic LCMV infection. PLoS Pathog. *14*, e1007053.

Rouse, B.T., and Sehrawat, S. (2010). Immunity and immunopathology to viruses: what decides the outcome? Nat. Rev. Immunol. *10*, 514–526.

Samuel, C.E. (2001). Antiviral actions of interferons. Clin. Microbiol. Rev. *14*, 778–809.

Speiser, D.E., Utzschneider, D.T., Oberle, S.G., Münz, C., Romero, P., and Zehn, D. (2014). T cell differentiation in chronic infection and cancer: functional adaptation or exhaustion? Nat. Rev. Immunol. *14*, 768–774.

Teijaro, J.R., Ng, C., Lee, A.M., Sullivan, B.M., Sheehan, K.C.F., Welch, M., Schreiber, R.D., de la Torre, J.C., and Oldstone, M.B.A. (2013). Persistent

LCMV infection is controlled by blockade of type I interferon signaling. Science *340*, 207–211.

Utzschneider, D.T., Charmoy, M., Chennupati, V., Pousse, L., Ferreira, D.P., Calderon-Copete, S., Danilo, M., Alfei, F., Hofmann, M., Wieland, D., et al. (2016). T cell factor 1-expressing memory-like CD8(+) T cells sustain the immune response to chronic viral infections. Immunity *45*, 415–427.

Wang, Y., Swiecki, M., Cella, M., Alber, G., Schreiber, R.D., Gilfillan, S., and Colonna, M. (2012). Timing and magnitude of type I interferon responses by distinct sensors impact CD8 T cell exhaustion and chronic viral infection. Cell Host Microbe *11*, 631–642.

Wherry, E.J., Blattman, J.N., Murali-Krishna, K., van der Most, R., and Ahmed, R. (2003). Viral persistence alters CD8 T-cell immunodominance and tissue distribution and results in distinct stages of functional impairment. J. Virol. *77*, 4911–4927.

Wilson, E.B., Yamada, D.H., Elsaesser, H., Herskovitz, J., Deng, J., Cheng, G., Aronow, B.J., Karp, C.L., and Brooks, D.G. (2013). Blockade of chronic type I interferon signaling to control persistent LCMV infection. Science *340*, 202–207.

Wu, T., Ji, Y., Moseman, E.A., Xu, H.C., Manglani, M., Kirby, M., Anderson, S.M., Handon, R., Kenyon, E., Elkahloun, A., et al. (2016). The TCF1-Bcl6 axis counteracts type I interferon to repress exhaustion and maintain T cell stemness. Sci. Immunol. *1*, eaai8593.

Xu, H.C., Grusdat, M., Pandyra, A.A., Polz, R., Huang, J., Sharma, P., Deenen, R., Köhrer, K., Rahbar, R., Diefenbach, A., et al. (2014). Type I interferon protects antiviral CD8+ T cells from NK cell cytotoxicity. Immunity *40*, 949–960.

Zinkernagel, R.M. (2005). Immunology and immunity against infection: general rules. J. Comput. Appl. Math. *184*, 4–9.

Zinkernagel, R.M., Planz, O., Ehl, S., Battegay, M., Odermatt, B., Klenerman, P., and Hengartner, H. (1999). General and specific immunosuppression caused by antiviral T-cell responses. Immunol. Rev. *168*, 305–315.

STAR★METHODS

KEY RESOURCES TABLE

REAGENT or RESOURCE	SOURCE	IDENTIFIER
Antibodies		
Anti-B220-FITC	Biolegend	CAT#103206; RRID:AB_312991
Anti-B220-PB	Biolegend	CAT#103227; RRID:AB_492876
Anti-CD4-BV605	Biolegend	CAT#100451; RRID:AB_2564591
Anti-CD44-AF700	Biolegend	CAT#103026; RRID:AB_493713
Anti-CD8a-BUV395	BD	CAT#563786; RRID:AB_2732919
Anti-CD8a-FITC	Biolegend	CAT#100706; RRID:AB_312745
Anti-CD8b-PerCP-Cy5.5	Biolegend	CAT#126610; RRID:AB_2260149
Anti-EOMES-PerCP-e710	Invitrogen	CAT#46-4875-82; RRID:AB_10597455
Anti-Fas-PE-Cy7	BD	CAT#557653; RRID:AB_396768
Anti-IFNg-PE	Biolegend	CAT#505808; RRID:AB_315402
Anti-Ki-67-APC	BD	CAT#561126; RRID:AB_10611874
Anti-LAG-3-BV421	Biolegend	CAT#125221; RRID:AB_2572080
Anti-mouse IgG2c-biotin	SOUTHERN BIOTECHNOLOGY	CAT#1077-08; RRID:AB_2794453
Anti-PD1-PE-Cy7	Biolegend	CAT#135216; RRID:AB_10689635
anti-Rabbit-IgG-A488	Invitrogen	CAT#A27034; RRID:AB_2536097
Anti-T-bet-APC	Biolegend	CAT#644814; RRID:AB_10901173
Anti-TCF-1	CST	CAT#2203S; RRID:AB_2199302
Anti-TIM3-BV421	Biolegend	CAT#119723; RRID:AB_2616908
Anti-TNFa-APC	Biolegend	CAT#506308; RRID:AB_315429
GL7-A647	Biolegend	CAT#144606; RRID:AB_2562185
Streptavidin-HRP	BD	CAT#554066
Anti-CD4 (for *In vivo* administration)	Leinco	CAT#C1333; RRID:AB_2737452
Anti-CD8 (for *In vivo* administration)	Leinco	CAT#C2442
Anti-IFNAR (for *In vivo* administration)	Leinco	CAT#I-401; RRID:AB_2491621
Anti-NK1.1 (for *In vivo* administration)	Leinco	CAT#N123; RRID:AB_2737553
Anti-PD-L1 (for *In vivo* administration)	BioXcell	CAT#BE0101; RRID:AB_10949073
Isotype control (for *In vivo* administration)	BioxCell	CAT#BE0090; RRID:AB_1107780
Bacterial and Virus Strains		
LCMV-Armstrong	Marco Colonna's Lab	N/A
LCMV-clone 13	Marco Colonna's Lab	N/A
Chemicals, Peptides, and Recombinant Proteins		
Brefeldin A	Biolegend	CAT#420601
H2-Db (LCMV gp33-41) tetramer	MBL International	CAT#TB-5002-1
H2-Db(LCMV gp276-284) tetramer	MBL International	CAT#TB-5009-1
Fetal Bovine Serum	Thermofisher	CAT#10437028
LCMV gp276-284 peptide	Genscript	CAT#RP19983
LCMV gp33-41 peptide	Genscript	CAT#RP20257
Linear Acrylamide	Ambion	CAT#AM9520
LIVE/DEAD Aqua	Invitrogen	CAT#L34966
RPMI-1640	Thermofisher	CAT#SH3009601
TMB Substrate Dako	Dako	CAT#T03026
Critical Commercial Assays		
Foxp3/transcription factor staining buffer	Thermofisher	CAT#00-5523-00
Luminaris Color HiGreen qPCR Master Mix	Thermofisher	CAT#K0394

(*Continued on next page*)

Continued

REAGENT or RESOURCE	SOURCE	IDENTIFIER
Negative Selection CD8 Kit	Biolegend	CAT#480008
qScript cDNA SuperMix	Quantabio	CAT#95048-100
Experimental Models: Cell Lines		
BHK cells	Marco Colonna's Lab	N/A
Vero Cells	Marco Colonna's Lab	N/A
Experimental Models: Organisms/Strains		
B6-CD45.1	Charles River	CAT#564
C57BL/6NCr	Charles River	CAT#556
Ifnar1–/–	Michael Diamond's Lab	N/A
Oligonucleotides		
GFP FWD primer: GACAACCACTACCTGAGCCA	Raju et al., 2018	N/A, Sigma Custom Synthesis
GFP REV primer: GTCCATGCCATGTGTAATCC	Raju et al., 2018	N/A, Sigma Custom Synthesis
LCMV gp FWD primer: CATTCACCTGGACTTTGTCAGACTC	McCausland and Crotty, 2008	N/A, Sigma Custom Synthesis
LCMV gp REV primer: GCAACTGCTGTGTTCCCGAAAC	McCausland and Crotty, 2008	N/A, Sigma Custom Synthesis
Software and Algorithms		
Prism, version 8	Graphpad	https://www.graphpad.com/scientific-software/prism/
Flowjo, version 10	FlowJo, LLC	https://www.flowjo.com/

LEAD CONTACT AND MATERIALS AVAILABILITY

This study did not generate new reagents. Further information and requests for resources and reagents should be directed to and will be fulfilled by the Lead Contact, Takeshi Egawa (egawat@wustl.edu).

EXPERIMENTAL MODEL AND SUBJECT DETAILS

Mice

Male C57BL/6N and B6-CD45.1 mice were purchased from Charles River Laboratory. *Ifnar1*$^{-/-}$ were obtained from Michael S. Diamond (Washington University). All mice were housed in a specific pathogen-free facility at Washington University in St. Louis, and were used at 8 to 10 weeks of age, unless stated otherwise. We used both males and females except that only male mice were used as recipient mice for bone marrow chimeras to minimize the risk of graft rejection due to the male antigen. All experiments were performed according to a protocol approved by Washington University's Animal Studies Committee.

METHOD DETAILS

Mouse Infection and Viral Load Quantification

Stocks of LCMV were made by propagating virus in BHK (baby hamster kidney) cells, followed by titering of culture supernatants by focus forming assay on Vero (African green monkey kidney) cells. For LCMV infection, mice were infected with 2×10^5 plaque-forming units (PFU) of LCMV-Arm via the intraperitoneal route or 2×10^6 (PFU) of LCMV-c13 by intravenous injection. For the quantification of plasma viral load, RNA was extracted from 10 μL of plasma using Trizol (Life Technologies). Before RNA extraction a spike-in of exogenous control mRNA encoding *clover* was added to the plasma samples as previously described. The amounts of the LCMV gp transcript relative to that of 'spiked- in' *clover* RNA were determined by real-time qRT-PCR using qScript cDNA synthesis and Luminaris HiColor Green Master Mix as previously described (Chou et al., 2016; McCausland and Crotty, 2008; Raju et al., 2018).

Antibody treatments

200 μg of anti-PD-L1 (29F.1.G2, BioXcell) was injected every day or every other day for treatments initiated on day 0, otherwise administration was every three days for a full two weeks of treatment. anti-IFNAR (MAR1, Leinco) was intraperitoneally injected at the indicated time points after infection at a dose of 1 mg. For depletion of CD4 T cells, 200 μg of anti-CD4 (GK1.5, Leinco) was injected on day −1 and +1 of infection. For depletion of CD8 T cells, 400 μg of anti-CD8 (YTS-169, Leinco) was injected on a day before infection. For NK cell depletion, 100 μg of anti-NK1.1 (PK136, Leinco) was injected on a day before infection.

Histology

Organs were fixed in 4% PFA overnight, then dehydrated in 70% ethanol. Samples were subject paraffin embedding and H&E staining using standard methods performed by the Developmental Biology Histology Core at Washington University in St. Louis. Images were collected using an EVOS FL Auto Imaging System (Thermofisher).

Cell Preparation, Staining, and Flow Cytometry

Single-cell suspensions were prepared by manual disruption of spleens with frosted glass slides. Absolute live cell counts were determined by Trypan-blue exclusion using Vi-Cell (Beckman Coulter). Tetramer staining was performed using iTag-PE LCMV gp33-44 and gp276-284 (MBL international) for 1 hour at RT followed by surface staining was performed at 4°C for 30 minutes. For intracellular cytokine staining, splenocytes were cultured in RPMI-1640 supplemented with 10% fetal bovine serum in the presence of 1 ug/ml of LCMV-gp peptide (Genscript) and 5 ug/ml of Brefeldin A (Biolegend) for 4 hours. Cells were stained for surface makers and then subject to LIVE/DEAD Aqua staining (Thermofisher) for 30 minutes at 4°C before being fixed with 4% PFA for 10 minutes at RT. Cells were then washed twice with 0.03% saponin in 2% FBS/PBS before being stained with the indicated antibodies in 0.3% Saponin in 2% FBS/PBS for 20 min at 4°C. Staining for transcription factors was performed using the Foxp3 staining kit (eBioscience) according to the manufacturer's instructions. Stained samples were analyzed with FACS LSR Fortessa or X20 (BD) and data processing with FlowJo Software (FlowJo. LLC).

Anti-LCMV antibody ELISA

Anti-LCMV antibody ELISA was performed as described previously (Raju et al., 2018). Briefly, Nunc Polysorp plates were coated with 10ug/mL sonicated cell lysate from LCMV-infected BHK-21 cells as capture antigen or uninfected BHK-21 cell lysate overnight followed by UV irradiation (300 mJ in Stratalinker 1800; Stratagene). Plasma antibody was detected with biotinylated anti-mouse IgG2c antibody (1077–08; Southern Biotech), followed by Streptavin-HRP (BD), and TMB substrate (Dako). Endpoint titers were calculated by a sigmoidal-dose response curve using Graphpad Prism software.

QUANTIFICATION AND STATISTICAL ANALYSIS

All statistical analyses were performed using Prism (Graphpad Software). *P*-values were calculated with an unpaired two-tailed Student's t test or the Mann-Whitney U-test for two-group comparisons and by one-way ANOVA for multi-group comparisons with the Tukey post hoc test. *$p < 0.05$; ** $p < 0.01$; *** $p < 0.001$; **** $p < 0.0001$.

DATA AND CODE AVAILABILITY

This study did not generate code or new datasets.

Cell Reports, Volume *29*

Supplemental Information

PD-1 Signaling Promotes Control of Chronic Viral Infection by Restricting Type-I-Interferon-Mediated Tissue Damage

Saravanan Raju, Daniel J. Verbaro, and Takeshi Egawa

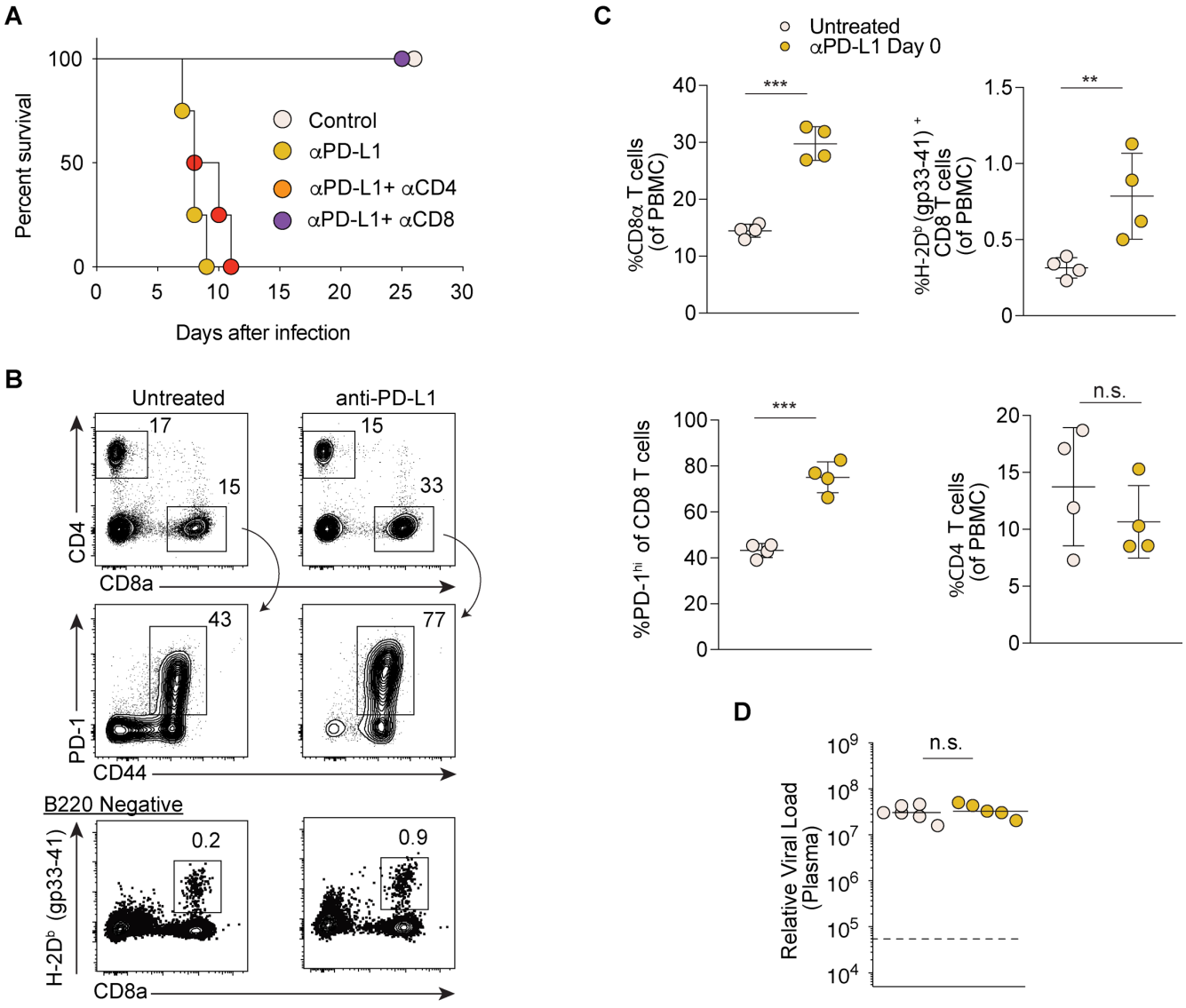

Figure S1. Anti-PD-L1 treatment initiated on day 0 of LCMV-c13 infection results in expansion of CD8 T cells with no impact on viral titer. Related to Figure 1. **(A)** Survival of LCMV-c13 infected mice that were treated with anti-PD-L1 on day 0 in the absence of $CD4^+$ or $CD8^+$ cells. **(B and C)** Expression of CD4, CD8a, CD44, PD-1, and gp33-specific TCR in peripheral blood mononuclear cells of B6 mice on 5dpi of LCMV-c13 with the indicated treatments. Representative plots (B) and data pooled from 3 experiments with n>4 mice per group shown with mean±SD (C). **(D)** Plasma LCMV *gp* transcripts in LCMV-c13-infected B6 mice with indicated antibody treatment on 5 dpi. Data were pooled from 2 independent experiments and shown with median. Statistical analysis tested with the Mann-Whitney U-test.

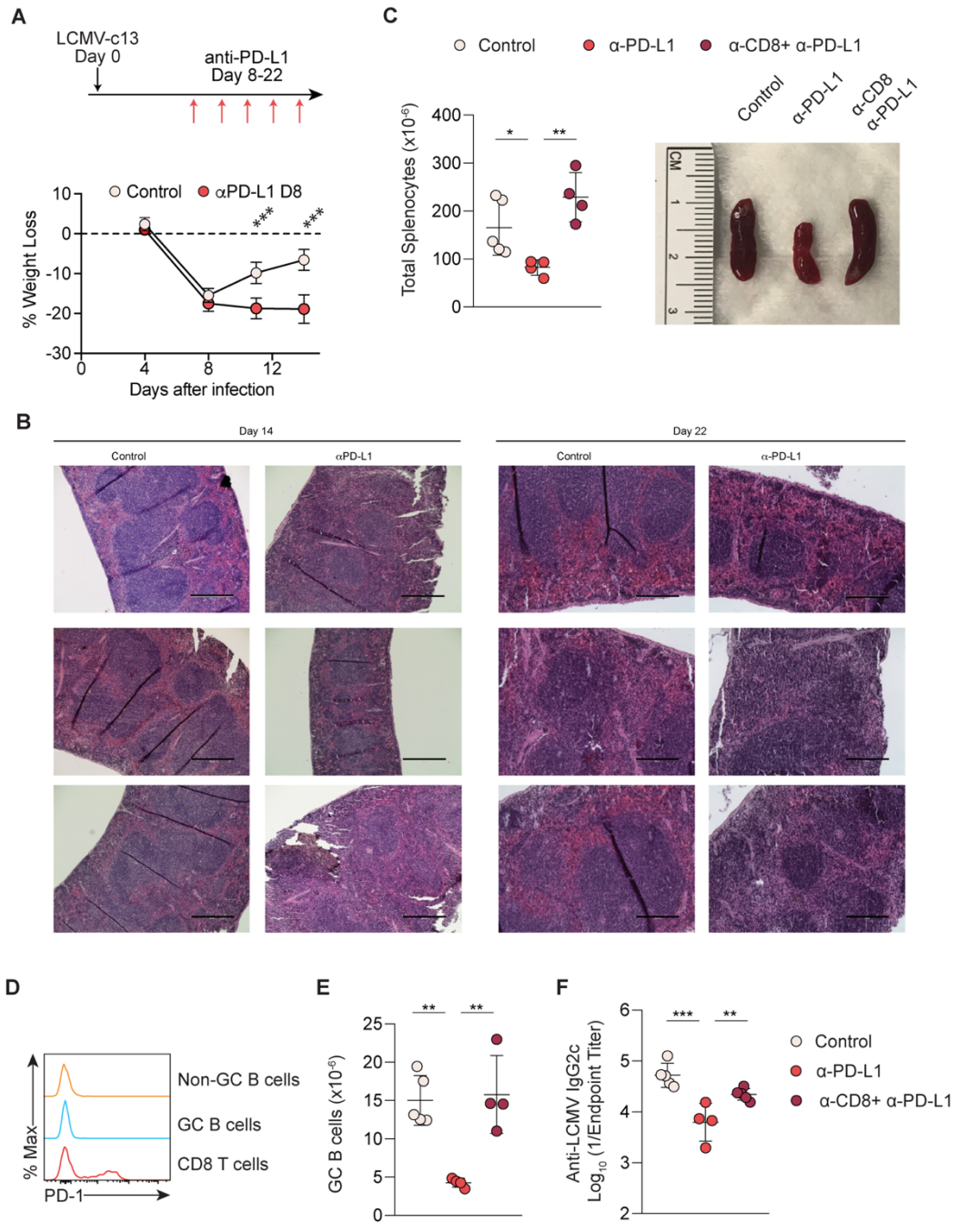

Figure S2. Non-lethal immunopathology following anti-PD-L1 treatment initiated on 8 dpi. Related to Figure 2. **(A)** Change in body weight following LCMV-c13 infection in control and B6 mice with anti-PD-L1 treatment initiated on 8 dpi. **(B)** Hematoxylin and eosin staining of spleen sections from control and day 8-22 anti-PD-L1-treated B6 mice on 14 dpi and 22 dpi as indicated. Scale bars indicate 400 μm. Images are representative of greater than 6 mice per group. **(C)** Splenocyte counts and gross appearance of the spleen of LCMV-c13 infected B6 mice on 22 dpi with treatment with anti-PD-L1 or anti-PD-L1+anti-CD8. **(D)** Expression of PD-1 by Fas^+ $GL7^+$ GC B cells, non-GC B cells and CD8 T cells in LCMV-c13 infected B6 mice on 22 dpi. **(E and F)** Absolute numbers of Fas^+ $GL7^+$ GC B cells in the spleen and anti-LCMV IgG2c antibody titers in the serum of LCMV-c13 infected, anti-PD-L1-treated B6 mice on 22 dpi. Data are pooled from two experiments with n>4 mice per group and shown with mean±SD.

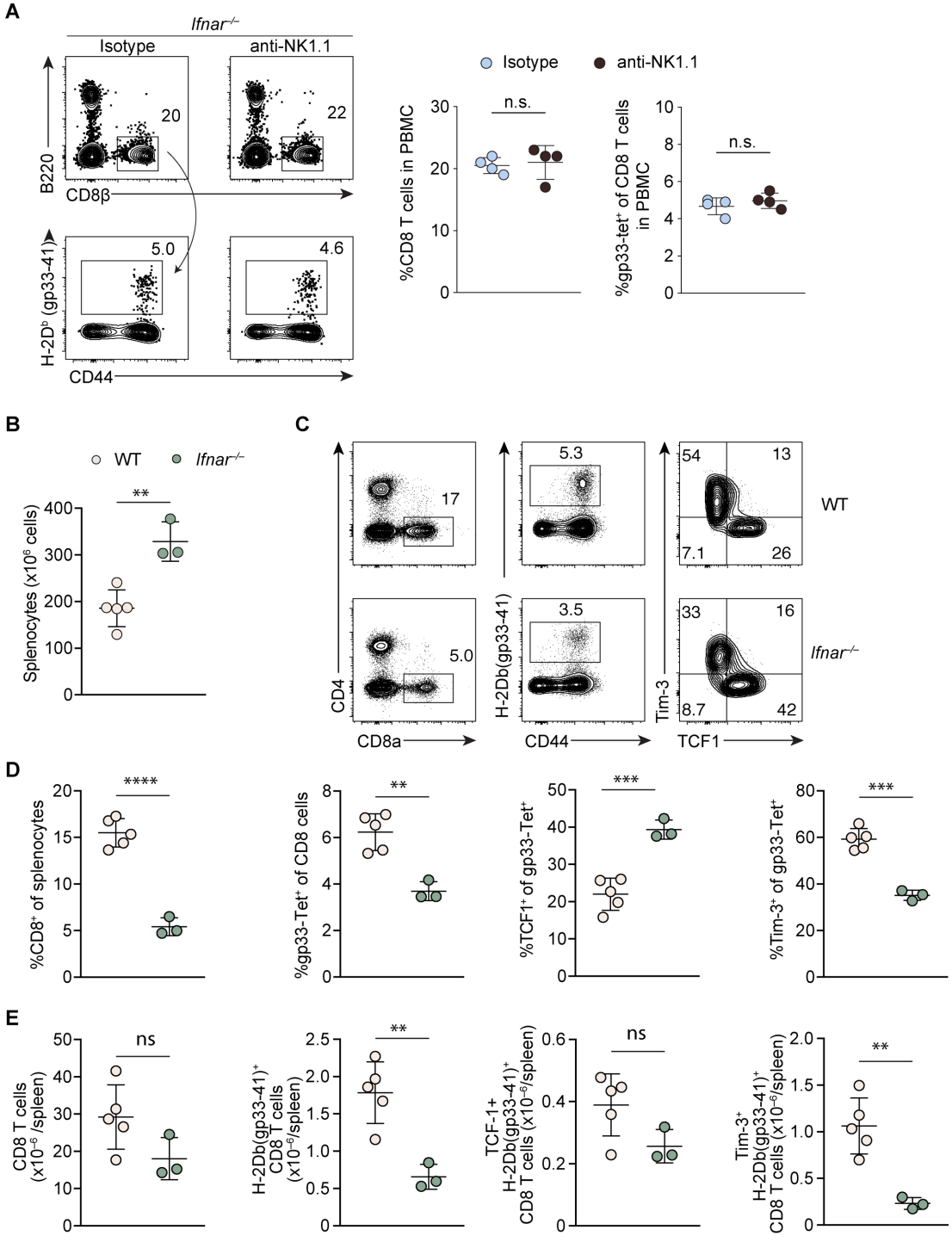

Figure S3. *Ifnar1*$^{-/-}$ mice display increased spleen size, but diminished CD8 T cell responses on 8 dpi of LCMV-c13. Related to Figure 4. **(A)** Frequencies of total and LCMV gp33-specific CD8 T cells in peripheral blood mononuclear cells on 22 dpi in *Ifnar1*$^{-/-}$ mice treated with anti-NK1.1 antibody. Data pooled from 2 experiments and shown with mean±SD. **(B and C)** Splenocyte counts (B) and expression of indicated molecules or tetramer binding by splenocytes (C) of *Ifnar1*$^{+/+}$ (WT, top) and *Ifnar1*$^{-/-}$ (bottom) mice on 8 dpi. Representative plots with the frequencies of cells in each gated population are shown. **(D and E)** Frequencies (D) and absolute numbers (E) of indicated populations in the spleen on 8 dpi pooled from 2 experiments and shown with mean±SD.

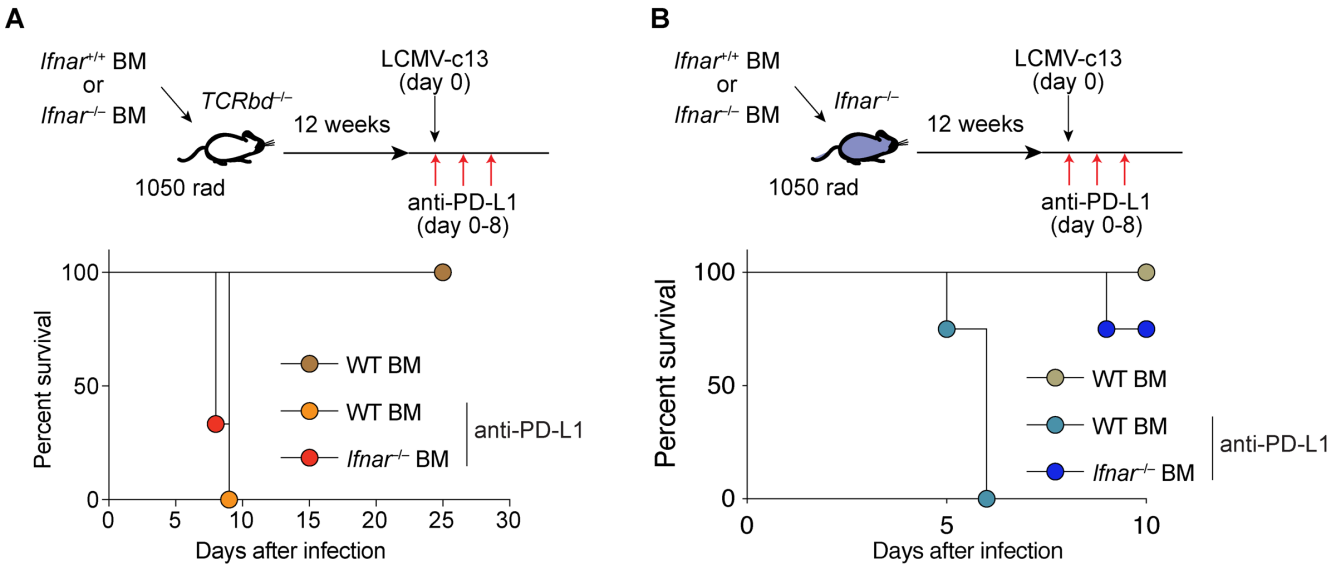

Figure S4. IFNAR signaling in either the hematopoietic or non-hematopoietic compartment is sufficient to cause lethal immunopathology. Related to Figure 4. Survival of *Ifnar1*$^{+/+}$ (A) and *Ifnar1*$^{-/-}$ (B) bone marrow (BM) chimeras reconstituted with *Ifnar1*$^{+/+}$ (WT) or *Ifnar1*$^{-/-}$ hematopoietic cells after infection with LCMV-c13 and treatment with anti-PD-L1 at the beginning of infection as indicated. Data are representative of two experiments with 5 mice in each group.